Preparation to the CMB PLANCK data analysis, bias due to the galactic polarized emissions

L. Fauvet, J.-F. Macías Pérez, F.-X. Désert
LPSC, Université Joseph Fourier Grenoble 1, CNRS/IN2P3,Institut National Polytechnique de Grenoble, 53 avenue des Martyrs,
38026 Grenoble cedex, France

The PLANCK satellite mission has been launched the 14th of May 2009 and is dedicated to the measurement of the Cosmic Microwave Background (CMB) in temperature and polarization. The presence of diffuse galactic polarized emission contaminates the measurement of the CMB anisotropies, in particular in polarization. Therefore a good knowledge of these emissions is needed to the accuracy required for PLANCK. In this context, we have developed and implemented a coherent 3D model of the two main polarized galactic emissions : synchrotron radiation and thermal dust. We have compared these models to the WMAP and ARCHEOPS data and to the 408 MHz all-sky continuum survey. From this, we are able to estimate the contribution of polarized foreground emissions to the polarized CMB radiation measured with PLANCK.

1 Introduction

The PLANCK satellite which is currently in flight, should give the most accurate measurement of the anisotropies of the CMB in temperature and polarization with a sensitivity of $2\mu K$ and an angular resolution of 5 arcmin [2]. It will cover a large range of frequencies between 30 and 857 GHz and it will allow us to study the Galactic microwave emissions. In order to obtain the optimal sensitivity it is necessary for us to estimate the foreground emissions and the residual contamination due to these foreground emissions. Indeed when, for the full sky, these emissions have the same order of magnitude than the CMB in temperature, they dominate by a factor 10 in polarization [2]. The principal polarized Galactic microwave emissions come from 2 effects : thermal dust emission and synchrotron emission. The synchrotron is well constrained by the 408 MHz all-sky continuum survey [8], by Leider between 408 MHz and 1.4 GHz [17], by Parkes at 2.4 GHz [5], by the MGLS *Medium Galactic Latitude Survey* at 1.4 GHz [16] and by the satellite WMAP *Wilkinson Microwave Anisotropies Probe* (see e.g. [9]). The synchrotron emission is due to ultrarelativistic electrons spiraling in a large-scale magnetic field. The thermal dust emission which has already been well constrained by IRAS [14], COBE-FIRAS [3] and ARCHEOPS [1], is due to dust grains which interact with the Galactic magnetic field and emit a polarized submillimetric radiation [3]. The polarization of these two types of radiation is orthogonal to the field lines. To obtain a realistic model of these emissions we must build a model based on a 3D modelisation of the Galactic magnetic field and the matter density in the Galaxy. The models are optimized with respect to preexisting data and can then be used to estimate the bias due to these emissions on the CMB measurement.

2 3D modelling of the Galaxy

A polarized emission can be described by the Stokes parameters I,Q and U [11]. For the polarized foreground emissions integrated along the line of sight we obtain, for synchrotron:

$$I_s = I_{\rm Has}\left(\frac{\nu_s}{0,408}\right)^{\beta_s}, \quad (1)$$

$$Q_s = I_{\rm Has}\left(\frac{\nu_s}{0,408}\right)^{\beta_s}\frac{\int\cos(2\gamma)p_s n_e\left(B_l^2+B_t^2\right)}{\int n_e\left(B_l^2+B_t^2\right)}, \quad (2)$$

$$U_s = I_{\rm Has}\left(\frac{\nu_s}{353}\right)^{\beta_s}\frac{\int\sin(2\gamma)p_s n_e\left(B_l^2+B_t^2\right)}{\int n_e\left(B_l^2+B_t^2\right)}, \quad (3)$$

where B_n, B_l and B_t are the magnetic field components along, longitudinal and transverse to the ligne of sight. p_s is the polarization fraction set to 75%. I_{Has} is the template map [8]. The maps are extrapolated at all the Planck frequencies using the spectral index β_s which is a free parameter of the model.

For the thermal dust emission :

$$I_d = I_{sfd}\left(\frac{\nu_d}{353}\right)^{\beta_d}, \quad (4)$$

$$Q_d = I_{sfd}\left(\frac{\nu_d}{353}\right)^{\beta_d}\int n_d\frac{\cos(2\gamma)\sin^2(\alpha)f_{\rm norm}p_d}{n_d}, \quad (5)$$

$$U_d = I_{sfd}\left(\frac{\nu_d}{353}\right)^{\beta_d}\int n_d\frac{\sin(2\gamma)\sin^2(\alpha)f_{\rm norm}p_d}{\int n_d}, \quad (6)$$

where the polarization fraction p_d is set to 10 %, β_d is the spectral index (set at 2.0) and f_{norm} is an empiric factor, fit to the ARCHEOPS data. The I_{sfd} map is the model 8 of [14].

The models are based on an exponential distribution of relativistic electrons on the Galactic disk, following [4], where the radial scale h_r is a free parameter. The distribution of dust grains n_d is also exponential [1]. The Galactic magnetic field is composed of two parts: a regular component and a turbulent component. The regular component is based on the WMAP team model [13] which is close to a logarithmic spiral to reproduce the shape of the spiral arms [7]. The pitch angle p between two spiral arms is a free parameter of the model. The turbulent component is described by a law of Kolmogorov [7] spectrum of relative amplitude A_{turb}.

3 Comparison to data

We computed Galactic profiles in temperature and polarization for various bands in longitude and latitude and various values of the free parameters. In order to optimize these 3D models we compare them to Galactic profiles computed using preexisting data using a χ^2 test. For the synchrotron emission in temperature, we use the 408 MHz all-sky continuum survey [8] as shown on Figure 1. In polarization we compared to the K-band WMAP 5 years data. The thermal dust emission model is optimized using the polarized ARCHEOPS data [1] at 353 GHz.

The best fit parameters for the 3D model in polarization are given in Table 1. The results are coherent for the 3 sets of data. In particular we obtain compatible results for the synchrotron and thermal dust emission models. A_{turb} and h_r are badly constrained as was already the case in Sun *et al* [15]. The best fit value of the pitch angle p is compatible with results obtained by other studies [15,13]. The best fit value for the spectral index of the synchrotron emission is lower than

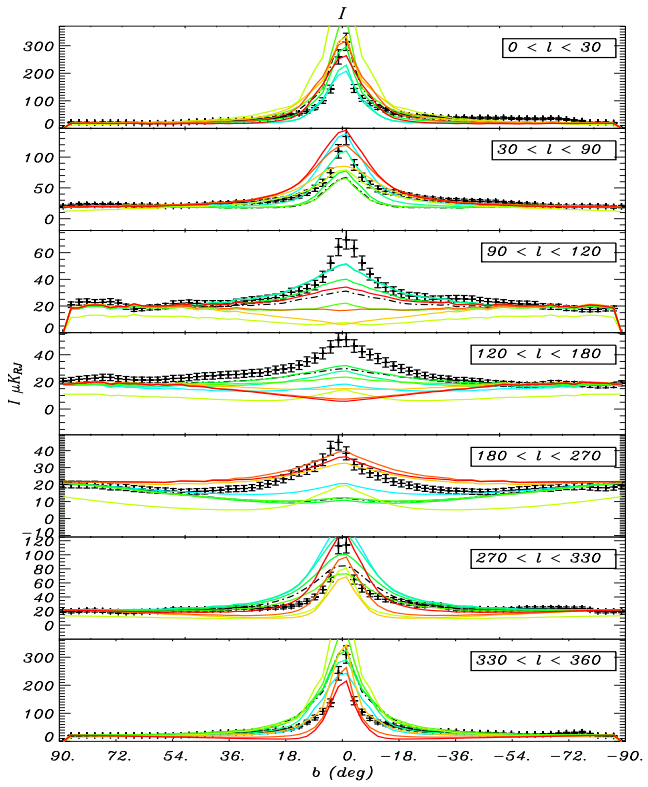

Figure 1: Galactic profiles in temperature at 408 MHz Haslam data in black and our synchrotron emission moedl for various values of the pitch angle p *(form green to red).*

the value found by [15,13], but this is probably due to the choice of normalisation for the regular componenent of the magnetic field. With these models we reproduce the global structure of the data (see for instance the Figure 1) appart from the Galactic center.

Table 1: Best fit parameters for synchrotron and thermal dust emission models.

	$p(deg)$	A_{turb}	h_r	β_s	χ^2_{min}
$WMAP$	$-30.0^{+40.0}_{-30.0}$	< 1.25 (95.4 % CL)	> 1 (95.4 % CL)	$-3.4^{+0.1}_{-0.8}$	5.72
$HASLAM$	$-10.0^{+70.0}_{-60.0}$	< 1.25 (95.4 % CL)	$5.0^{+15.0}_{-2.0}$	$\emptyset$	5.81
$ARCHEOPS$	-20^{+80}_{-50}	$< 2.25(95.4\%CL)$	$\emptyset$	$\emptyset$	1.98

4 Conclusions

From the above best fit parameters we estimate the contamination of the CMB PLANCK data by the polarized galactic emissions. We compared power spectra computed with simulations of the CMB PLANCK data [a]. Figure 2 shows the temperature and polarization power spectra at 143 GHz for the CMB simulation (*red*) and the Galactic foreground emissions applying a Galactic cut $|b| < 15deg$ (*black*). The foreground contamination seems to be weak but for the BB modes an accurate foreground substraction is extremely important for the detection of the primordial gravitational waves. More details can be found in [6].

[a] We used cosmological parameters for a model ΛCDM like proposed in [10] with a ratio tensor-scalar of 0.03.

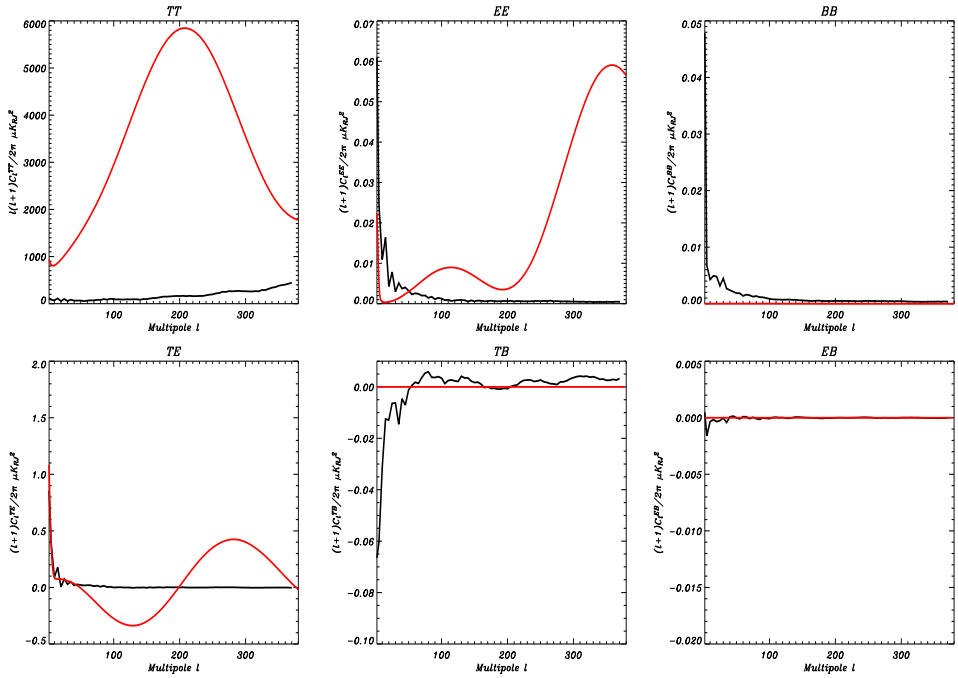

Figure 2: Clockwise from top left : power spectra C_l^{TT},C_l^{EE},C_l^{BB},C_l^{TE},C_l^{TB},C_l^{EB} at 143 GHz for $|b| < 15deg$ (see text for details).

References

1. A. Benoît *et al*, A&A **424**, 512 (2004)
2. The Planck Consortia, 2004, *Planck : The Scientific Program*
3. F. Boulanger *et al*, A&A **312**, 256 (1996)
4. R. Drimmel & D.N. Spergel, ApJ **556**, 181 (2001).
5. A. Duncan et al, A. & A. **350**, 447 (1999).
6. L. Fauvet, J.F. Macías-Pérez *et al.*, **astro-ph/1003.4450**.
7. J. L. Han *et al*, A&A **642**, 868 (2006).
8. C.G.T Haslam et al*et al*, A&AS **47**, 1 (1982).
9. G. Hinshaw *et al*, ApJS **170**, 288 (2007).
10. E. Komatsu *et al*, ApJS **180**, 306 (2009)
11. A. Kosowsky, Ann. Phys. **246**, 49 (1996).
12. M. -A. Miville-Deschênes *et al*, A&A accepted **astro-ph/08023345**, 2008 (.)
13. L. Page *et al*,ApJSS **170**, 335 (2007).
14. D. J. Schlegel, D. P. Finkbeiner & M. Davies, ApJ **500**, 525 (1998).
15. X.H. Sun *et al*,A &A manuscrit **astro-ph/0711.1572v1**, 2008 (.)
16. B. Uyaniker *et al*, A & A.S.S. accepted **astro-ph/9905023v1**, 1999 (.)
17. M. Wolleben *et al*, A.& A. **448**, 411 (2006).